JSST
Journal of Space Science and Technology

P-ISSN: 2008-4560
E-ISSN: 2423-4516

Journal of Space Science and Technology

Vol. 17, Special Issue, pp. 45-58, 2024
https://doi.org/10.22034/jsst.2024.1509
Journal Homepage: https://jsstpub.com

Original Research Paper

Finite-Time Disturbance Observer Based Fractional Order Nonsingular Terminal Sliding Mode Attitude Control of Satellites

Shirkoo Piri, Jalil Beyramzad, and Esmaeel Khanmirza*

School of Mechanical Engineering, Iran University of Science and Technology, Tehran, Iran

ARTICLE INFO

Article History:

Received 30 November 2024
Revised 16 December 2024
Accepted 23 December 2024
Available Online 27 December 2024

Keywords:

Fractional order SMC
Attitude control
Satellite
Disturbance observer
Terminal sliding mode
Finite-time stability

ABSTRACT

This study presents a method for implementing rigid satellite output feedback control that considers dynamic uncertainties and external disturbances, all while avoiding the need for velocity state measurement. The dynamics of a rigid satellite are first represented using the modified Rodrigues parameter (MRP) and then transformed into Euler-Lagrangian form to provide the state-space representation of the dynamics. The availability of angular velocity data for practical applications is often limited by cost or technical limitations. Consequently, angular velocity is considered to be immeasurable. In order to minimize the need for extra mathematical calculations and the creation of separate observers to estimate uncertainties and system states, a finite time disturbance observer (third order sliding mode (TOSM) observer) was used to simultaneously estimate both uncertainties and system states. The main component of the suggested controller incorporates the fractional order nonsingular terminal sliding mode technique, which guarantees stability within a finite time and avoids chattering. The simulation results of the proposed methodology have been presented and compared with the results of techniques available in the literature, showcasing the efficacy of the method described in this study and the enhancement of the findings of previous relevant research.

*Corresponding Author's E-mail: khanmirz@iust.ac.ir

How to Cite this Article:
Sh. Piri, J. Beyramzad and E. Khanmirza, "Finite-time disturbance observer based fractional order nonsingular terminal sliding mode attitude control of satellites," *Journal of Space Science and Technology*, Vol. 17, Special Issue, pp. 45-58, 2024, https://doi.org/10.22034/jsst.2024.1509.

1. INTRODUCTION

For a spacecraft's attitude control system to be deemed appropriate for space missions, it must meet rigorous performance criteria. The challenge of managing a satellite's orientation is both significant and pragmatic. The significance of this function in many space operations, such as satellite surveillance, space station docking and installation, and spacecraft formation flying [1], is likely the reason for the interest in this function. Over the last several decades, much study has been carried out on various approaches to address the problem. The tactics include classic linear control, optimal control, model predictive control, nonlinear control approaches, and intelligent control strategies. It is important to note that most current spacecraft attitude control algorithms rely on having accurate and immediate measurement data for both attitude orientation and angular velocity [1]. Nevertheless, the availability of angular velocity data for practical purposes may be limited due to financial limitations or implementation limitations. Microsatellites, for instance, may not have the capability to gather data on angular velocity. Implementing partial state feedback attitude control systems for spacecraft is attractive due to the practical factor involved. This difficulty, which involves the lack of easily available velocity measurement data, has been extensively examined in previous research. Several methods have been proposed in the literature to develop attitude controllers that do not rely on angular velocity [1-6]. Sliding mode control (SMC) is a popular option among the several methods available for addressing issues related to the control of aeronautical systems. Many academics have used sliding mode control (SMC) for controlling uncertain systems because of its rapid dynamic response, ability to handle lumped uncertainty, and comparatively simple design approach. Despite the many benefits, using a linear sliding function in conventional sliding mode control leads to the inability to guarantee the finite-time convergence of the system's state error. However, this remains the case despite the many benefits. To bypass this limitation, researchers have developed a technique called terminal sliding mode control (TSMC). Instead of using a linear sliding function [7-9], this technique employs nonlinear sliding functions throughout the design phase. TSMC achieves enhanced accuracy and rapid convergence via meticulous parameter configuration. However, conventional TSMC exhibits two significant constraints: 1) SMC exhibits a faster convergence time compared to the current method. 2) The current method encounters a singularity problem. Numerous significant investigations have been carried out to address these shortcomings. The use of fast TSMC (FTSMC) in combination with nonsingular TSMC (NTSMC) resolved every problem. To simultaneously tackle both of these problems, a method called nonsingular fast TSMC (NFTSMC) has been developed. The NFTSMC controller has been extensively used in various systems due to its exceptional features, such as finite-time stability, singularity removal, high tracking performance, and robustness against uncertainties. These attributes have enabled the NFTSMC to effectively rival other control methods [9].

Chattering arises due to the use of a switching gain in both classic SMC and NFTSMC during the reaching phase, combined with a substantial fixed sliding gain, in order to mitigate the impact of lumped uncertainty. The system is negatively affected, hence reducing the efficacy of both control mechanisms indicated before.

Control approaches such as FTSMC or NTSMC have focused only on addressing specific vulnerabilities, disregarding the other weaknesses of the regular SMC. NFTSMC has the potential to rectify many limitations associated with traditional SMC or alternative control methods based on TSMC. However, including a high-frequency reaching control term into the control input of the aforementioned systems, such as TSMC, FTSMC, NTSMC, and NFTSMC, does not effectively reduce chattering. Consequently, several valuable control systems using high-order sliding mode control (HOSMC) have been suggested [10-11].

In recent years, there has been a significant amount of research conducted on applying control techniques based on terminal sliding mode to regulate the state of satellites [13-17]. This is due to the multiple benefits associated with these approaches.

Two challenging components of developing a control system using SMC or TSMC are understanding the boundaries of external disturbances and dynamic uncertainties, as well as creating a precise dynamic model. These factors are not predetermined for real-world systems. Several computer methods have been devised to estimate

this undisclosed model, such as different forms of neural networks and fuzzy logic systems [18]. Nevertheless, to successfully finalize the design process, controller designers need access to precise velocity data, which is often unattainable in a functioning system owing to limitations imposed by cost and space restrictions. Thus, if state feedback strategies are employed for controller design methods, the aforementioned control systems are not feasible for practical implementation. Instead, output feedback strategies must be utilized to ensure practical implementation of the designed control system.

To reduce or eliminate the chattering phenomenon, one might decrease the sliding gain of the switching element[12]. This is the core principle of the solution. Therefore, in order to account for the uncertainties, it is necessary to adjust the control signals by either fully or partially estimating the uncertainties. To address the estimated error caused by uncertainty, the switching element is now used. In order to achieve the sliding mode, the sliding gain will be adjusted to a lower value compared to the prior technique. The severity of the chattering phenomenon will decrease, depending on the precision of the estimating technique.

Several academics have recently integrated fractional calculus with various control approaches, such as TSM and NTSM controllers. Fractional-order controllers provide more flexibility in adjusting the time and frequency response of the closed-loop system. However, this is contingent upon their possessing a higher number of degrees of freedom (DOF) compared to their integer-order counterparts. Within the control world, fractional calculus is recognized as a potent tool that offers additional degrees of freedom, namely the order, which in turn allows for more flexibility in designing controllers with integer orders [19-20]. The use of fractional derivatives and integrals in sliding surfaces has several benefits, including strong resilience against uncertainties and external disturbances, enhanced reaction speed, avoidance of singularities, and rapid convergence rate [21]. Furthermore, extensive verification has shown that the fractional-order SM (FOSM) is capable of enhancing tracking and anti-disturbance performance when compared to the integer-order SM [19-21]. While these innovative controllers provide certain advantages in terms of delivering stability within a specific time frame, several studies fail to analytically analyze the stability and boundedness of the error signals after they reach the sliding surface. In other cases including a thorough stability investigation, the control rule often incorporates a fractional-order differentiator. Because the boundedness of the fractional-order differentiator has not been examined, the control law's boundedness cannot be completely ensured, unlike the fractional-order integrator. In addition, the use of FOSM controllers for spacecraft attitude control is limited, despite their many advantages. Several studies have shown that the use of a fractional-order controller (FOC) may improve the performance of control systems [19-20].

The basics of fractional order calculation, numerical calculations related to it, as well as their application in the design of fractional order control systems, have been discussed in detail in references [22-23], which can be referred to for further study.

Several model-based strategies have been proposed in the literature to estimate the uncertainty of dynamic systems, including time delay estimation method-based observer, neural networks and fuzzy logic-based observer, second-order, third-order or in general high order sliding mode observers, and extended state observer [18]. Since the TDE approach is limited to estimating the capacity of unknown inputs, an additional observer is necessary to estimate the velocities of the system. It increases the complexity of the system and contributes to the duration required for computation. The neural observer's ability to acquire knowledge and provide exceptional approximations enables it to supply estimated data with unlimited accuracy. Specifically, it must have the capability to estimate both the overall uncertainty and the velocities of the system. Consequently, the system depends on a solitary observer. Although the use of learning techniques might enhance long-term performance, the need for an online learning mechanism may impede the system's immediate performance in the face of external disruption [18-24].

The ability to implement such a system in real-world scenarios is also impeded by the intricacy of training neural network weights, which requires substantial computer resources.

Observers using fuzzy logic encounter comparable difficulties to those employing neural networks. In conclusion, it can be said that intelligent learning methods have the capability to

assess the uncertainty in the system. However, their implementation is complex due to the involvement of several weighting elements or fuzzy rules. Although traditional extended state observers possess the capability to estimate system states and uncertainty using a single observer, they suffer from inaccuracies and the estimation process is not finite time.

The second-order sliding mode (SOSM) observer is distinguished from other observers by its capability to estimate system velocities and uncertainties using finite-time error estimates [25]. This confers a competitive edge to the SOSM observer. The SOSM observer's output injection, used to estimate uncertainty, has a discontinuous term that leads to an unpleasant chattering phenomenon [18,24-26]. However, it is important to note that the velocity prediction produced using this approach is very precise and demonstrates little chattering compared to other methods. To restore the uncertainty, it is necessary to use a low-pass filter [18,24-26]. Conversely, this leads to a delay in the estimating process and a decrease in the accuracy of the SOSM observer's estimations. The third-order sliding mode (TOSM) observer, in comparison to the SOSM observer, offers improved estimation accuracy and less chattering when estimating lumped uncertainty. Furthermore, the TOSM observer retains almost all of the advantages linked to the SOSM observer. The TOSM observer has gained popularity among several experts [18,24-26] because of its significant benefits in regulating uncertain systems.

Consequently, recent studies have focused on the TOSM observer, which can provide a consistent output injection. Consequently, the compulsory filtering that was part of the SOSM observer has been eliminated. In the current study, the TOSM observer was used to determine both the velocities and uncertainties of rigid spacecraft systems, without the need for any filtering methods. Once convergence occurs, the anticipated velocity is replaced by the actual velocity signal. As a consequence, the design of the controller becomes more streamlined.

This work proposes the use of a fractional-order NTSMC as a way for accurate attitude control of rigid spacecraft, based on the acquired information from disturbance observer. The proposed approach obviates the necessity for real-time data on the system's velocity by leveraging an observer.

This proposed control approach allows us to get a control law that has desired attributes, including robustness in the presence of errors, high accuracy, non-singularity, removal of chattering, and finite-time stability, all without the need for angular velocity measurement.

2. MRP-BASED ATTITUDE DYNAMICS

The literature has extensively discussed the dynamics and kinematics of satellites, using several methodologies, each with its own advantages and disadvantages. Various methods, such as Eulerian angles, Euler-Rodrigues parameters (in Quaternion formulation), Cayley-Klein parameters, and Cayley-Rodrigues parameters, are used to describe the movement and behavior of satellites. Most control applications need parameterizations where the singularity is located at a significant distance from the origin. The assessment of attitude often uses the quaternion representation as a parameterization. When manipulating quaternions, the kinematic equations exhibit linearity concerning angular velocities, and there are no instances of singularities for any rotation of the Eigen axis in combination with an algebraic attitude matrix. Due to the use of four components in the quaternion parameterization to depict attitude motion, the quaternion components are neither minimum nor independent. Therefore, it is necessary for the quaternion to possess a norm of one [13-14].

In addition, the use of quaternion representation in the kinematic equations eliminates the possibility of singularities. However, due to the additional parameters needed for quaternions, this parameterization strategy is not minimal. Recently, the modified Rodrigues parameters (MRP) have been used in spacecraft control applications due to their ability to allow rotations of up to 360 degrees [13-14]. The Rodrigues parameters provide a concise representation in three dimensions. Regrettably, the presence of a singularity while performing 180-degree rotations makes this parameterization challenging to use for really large degrees of rotation. Employing rotations of fewer than 180 degrees in each consecutive revolution may perhaps help address this problem. The use of this portrayal of attitude yields the following advantages: The parameters enable rotations of 360 degrees and provide a basic parameterization.

Constructing observers and estimators to estimate satellite attitude is often essential. Utilizing the modified Rodrigues parameters technique, instead of the quaternion method, would streamline the mathematical control design process and reduce computational requirements. In the current work, we will use this modeling method to analyze and describe the satellite's dynamics and kinematics concerning the controller being examined.

In the event where $\sigma \in \mathcal{R}^3$ stands in for the MRP, as specified by [13-14], then we have:

$$\sigma = [\sigma_1 \quad \sigma_2 \quad \sigma_3]^T = \hat{e} \tan\frac{\theta}{4} \tag{1}$$

Where $\hat{e} = [e_1 \quad e_2 \quad e_3]$ is a rotation around the central axis and is a rotation about the Euler axis in the body frame. Here is a σ based description of the system's attitude kinematics:

$$\dot{\sigma} = \Gamma(\sigma)\omega \tag{2}$$

Where ω represents the angular velocity components expressed in a body axis frame $[x \quad y \quad z]$ relative to an inertial frame $[X \quad Y \quad Z]$ and $\Gamma(\sigma)$ equation is as follows [12-14]:

$$\Gamma(\sigma) = \frac{1}{4}[(1-\sigma^T\sigma)I_{3\times3} + 2S^*(\sigma) + 2\sigma\sigma^T] \tag{3}$$

$I_{3\times3}$ is the identity matrix, while the matrix $S^*(\sigma)$ is a skew-symmetric matrix written in the following form [15]:

$$S^*(\sigma) = \begin{bmatrix} 0 & -\sigma_3 & \sigma_2 \\ \sigma_3 & 0 & -\sigma_1 \\ -\sigma_2 & \sigma_1 & 0 \end{bmatrix} \tag{4}$$

When the control inputs $u(t) \in \mathcal{R}^3$ and the external disturbances $d(t) \in \mathcal{R}^3$ are taken into consideration, the dynamics of the rigid spacecraft may be represented as follows [13-15]:

$$J\dot{\omega} = -S^*(\omega)J\omega + u(t) + d(t) \tag{5}$$

Where $J \in \mathcal{R}^3$ refers to the matrix that represents the moment of inertia and $S^*(\omega)$ refers to the skew-symmetric matrix that represents the angular velocity. The following is a Lagrangian version of the dynamics of the spacecraft's attitude stabilization [13-15], which is derived by using Equations (2) and (5):

$$M(\sigma)\ddot{\sigma} + C(\sigma,\dot{\sigma})\dot{\sigma} = \tau + \tau_{ext} \tag{6}$$

Different components of the aforementioned equation may be written as follows:

$$M(\sigma) = \Gamma(\sigma)^{-T}J\Gamma(\sigma)^{-1} \tag{7}$$

$$C(\sigma,\dot{\sigma}) = -\Gamma(\sigma)^{-T}J\Gamma(\sigma)^{-1}\dot{\Gamma}(\sigma)\Gamma(\sigma)^{-1} - \Gamma(\sigma)^{-T}S^*(J\omega)\Gamma(\sigma)^{-1} \tag{8}$$

$$\tau = \Gamma(\eta)^{-T}u(t) \tag{9}$$

$$\tau_{ext} = \Gamma(\eta)^{-T}d(t) \tag{10}$$

The state space form of dynamic equations is often utilized in controller design for nonlinear systems. With the assumptions of $x_1 = \sigma$ and $x_2 = \dot{\sigma}$, the satellite dynamic equations may be written in the following state space form:

$$\begin{cases} \dot{x}_1 = x_2 \\ \dot{x}_2 = f(x) + g(x)u + d^* \end{cases} \tag{11}$$

Where $f(x) = M^{-1}(\sigma)C(\sigma,\dot{\sigma})\dot{\sigma}$, $g(x) = M^{-1}(\sigma)\Gamma(\sigma)^{-T}$ and $d^* = M^{-1}(\sigma)\Gamma(\sigma)^{-T}d(t)$

Whereas d^* is the unknown bounded external disturbances $|d^*| \le \delta_d$. The two functions represented by $f(x)$ and $g(x)$ are considered here, each of which may be expressed as the sum of a nominal function and an unknown but limited uncertainty:

$$\begin{cases} f(x) = f_0(x) + \Delta f(x); |\Delta f(x)| \le \delta_f \\ g(x) = g_0(x) + \Delta g(x); |\Delta g(x)| \le \delta_g \end{cases} \tag{12}$$

Using Eq. (12) in place of Eq. (11), we get:

$$\begin{cases} \dot{x}_1 = x_2 \\ \dot{x}_2 = f_0(x,t) + g_0(x,t)u + \Delta(x,t) \\ y = x \end{cases} \tag{13}$$

The system total lumped uncertainty is denoted by $\Delta(x,u,t) = \Delta f(x) + \Delta g(x)u + d^*$. With the assumption of a maximum value for the control inputs $|u| \le \delta_u$, the following may be written:

$$|\Delta(x,t)| \le |\Delta f + \Delta g\delta_u + \delta_d| \le |\delta_f + \delta_g\delta_u + \delta_d| \le \Delta_D \tag{14}$$

3. CONTROLLER DESIGN

To design the controller, we first define the sliding surface as follows:

$$s = e + \frac{1}{\lambda} sig(\dot{e})^{\eta} \quad (15)$$

Where $sig(\dot{e})^{\eta} = |\dot{e}|^{\eta} sign(\dot{e})$, and $1 < \eta < 2$. Once $s = 0$ is achieved, the sliding mode surface Eq. (18) may be expressed in the following manner:

$$0 = e + (1/\lambda) sig(\dot{e})^{\eta} \quad (16)$$

The time T_s required for the tracking error $e(t)$ to approach zero is provided in reference [27]:

$$T_s = \frac{max(e(0))^{(1-1/\eta)}}{\lambda^{(1/\eta)}(1 - 1/\eta)} \quad (17)$$

Once the appropriate sliding surface, as defined by Eq. (18), has been determined, the subsequent task is to develop a NTSMC that will guide system of Eq. (13) towards this sliding surface. As per the sliding mode design approach, the control input u is composed of two components $u = u_{eq} + u_{SMC}$. The equivalent control, denoted as u_{eq}, is derived by solving the equation $\dot{s} = 0$ for the nominal system, disregarding any errors or external disturbances. By differentiating Eqs. (15) concerning time, one obtains:

$$\dot{s} = \dot{e} + \frac{\eta}{\lambda} |\dot{e}|^{\eta-1} \ddot{e} \quad (18)$$

By rewriting Eqs. (13), $\ddot{e}$ becomes:

$$\ddot{e} = f_0(x,t) + g_0(x,t)u(t) + \Delta(x,t) - \ddot{x}_d(t) \quad (19)$$

By replacing the Eqs. (19) with Eqs. (18), we get:

$$\dot{s} = \dot{e} + \frac{\eta}{\lambda} |\dot{e}|^{\eta-1} (f_0(x,t) + g_0(x,t)u(t) + \Delta(x,t) - \ddot{x}_d(t)) \quad (20)$$

Given the constraint $\dot{s} = 0$, one can choose the appropriate control law as:

$$u_{eq} = \frac{1}{g_0(x,t)} \left(\ddot{x}_d(t) - f_0(x,t) - \frac{\lambda \dot{e}}{\eta} |\dot{e}|^{1-\eta} \right) \quad (21)$$

The switching control is constructed in the following manner:

$$u_{SW} = -\frac{1}{g_0(x,t)} (K \text{sign}(s)) \quad (22)$$

Next, the overall control u is determined:

$$u = u_{eq} + u_{SW} = \frac{1}{g_0(x,t)} \left(\ddot{x}_d(t) - f_0(x,t) - \frac{\lambda \dot{e}}{\eta} |\dot{e}|^{1-\eta} - K sign(s) \right) \quad (23)$$

3.1 Design of FO-NTSMC

For the design of FO-NTSMC, some of the main concepts of fractional order calculus are explained below.

A fractional operator is a generalization of the differential and integral operators, indicated by the fundamental operators ${}_{t_0}D_t^{\alpha}, {}_{t_0}I_t^{\alpha}$. These operators have a simple formulation as follows:

Definition 1. Function $x(t)$'s α -order Riemann-Liouville fractional integration may be expressed as

$${}_{t_0}I_t^{\alpha} x(t) = \frac{1}{\Gamma(\alpha)} \int_{t_0}^{t} (t-s)^{\alpha-1} x(s) ds \quad (24)$$

Given that $\alpha \in R^+$, t_0 represents the starting time, and $\Gamma(\alpha)$ refers to Euler's Gamma function:

$$\frac{d^{\alpha} x(t)}{dt^{\alpha}} = {}_{t_0}D_t^{\alpha} x(t) = \frac{1}{\Gamma(m-\alpha)} \frac{d^m}{dt^m} \int_{t_0}^{t} (t-s)^{m-\alpha-1} x(s) ds \quad (25)$$

That is, m is the first integer greater than α, where $m - 1 \leq \alpha < m$.

Definition 2. The function $x(t)$'s α -order Caputo fractional derivative is expressed as:

$${}_{t_0}D_t^{\alpha} x(t) = \frac{d^{\alpha} x(t)}{dt^{\alpha}} = \frac{1}{\Gamma(m-\alpha)} \int_{t_0}^{t} (t-s)^{m-\alpha-1} \frac{d^m}{ds^m} x(s) ds \quad (26)$$

Where m is first integer greater than α. For the Riemann–Liouville derivative, the following equivalence is true:

$${}_{t_0}I_t^{\alpha} \left({}_{t_0}D_t^{\alpha} x(t) \right) = x(t) - \sum_{i=1}^{m} \left[{}_{t_0}I_t^{i-\alpha} x(t) \right]_{t=t_0} \frac{(t-t_0)^{\alpha-i}}{\Gamma(\alpha - i + 1)} \quad (27)$$

Assumed that $x(t)$ is a function with integrable fractional derivative ${}_{t_0}D_t^{\alpha} x(t)$ $(m - 1 \leq \alpha < m)$.

Lemma 1 [30]**.** The operator ${}_{t_0}I_t^{\alpha}$, which represents fractional integration, is bounded and adheres to the following approximation$\| {}_{t_0}I_t^{\alpha}x\| \leq B \| x \|$.

Theorem 1 [28]: Consider $x = 0$ as a point of equilibrium for the nonautonomous fractional-order system ${}_{t_0}D_t^{\alpha} = f(x,t)$, where $f(x,t)$ fulfills the Lipschitz condition with a Lipschitz constant$l > 0$. Let us pretend that there is a Lyapunov function $V(t,x)$ that meets:

$$\alpha_1 \| x \| \leq V(t,x) \leq \alpha_2 \| x \| \text{ and } \dot{V}(t,x) \leq -\alpha_3 \| x \| \tag{28}$$

Where $\alpha \in (0,1)$ and $\alpha_i \in R^+, i = 1,2,3$. Subsequently, the system's equilibrium point attains asymptotic stability.

Theorem 2 [29]: Assume that $x = 0$ is an equilibrium point for fractional order non-autonomous system ${}_{t_0}D_t^{\alpha} = f(x,t)$, where $f(x,t)$ applies in Lipschitz conditions with Lipschitz constant $l > 0$. And there is a Lyapunov function like $V(t,x)$ that applies in the following condition:

$$\alpha_1(\| x \|) \leq V(t,x) \leq \alpha_2(\| x \|) \text{ and } {}_{t_0}D_t^{\alpha}V(t,x) \leq -\alpha_3(\| x \|) \tag{29}$$

Now, to design FO-NTSMC, we define the sliding surface as follows.

$$s = {}_{t_0}D_t^{\alpha}e + \frac{1}{\lambda}sig(\dot{e})^{\eta} \tag{30}$$

Where $\eta \in (1,2)$, λ is a specified positive constant, and ${}_{t_0}D_t^{\alpha}$ is the fractional derivative of order $\alpha \in (0,1)$. By dividing the tracking error definition by Eq. (30) and adding it to Eq. (13), we get:

$$\dot{s}(t) = {}_{t_0}D_t^{\alpha+1}e(t) + \frac{\eta}{\lambda}\ddot{e}(t)|\dot{e}|^{\eta-1} = {}_{t_0}D_t^{\alpha+1}e(t) + \frac{\eta}{\lambda}|\dot{e}|^{\eta-1}(f_0(x,t) + g_0(x,t)u + \Delta(x,t) - \ddot{x}_d) \tag{31}$$

In order to get the equivalent control set $\dot{s} = 0$, the necessary response may be accomplished by selecting the control law as $u = u_{eq} + u_{SW}$, where:

$$u_{eq} = \frac{1}{g_0(x,t)}\left(\ddot{x}_d(t) - f_0(x,t) - \frac{\lambda}{\eta}\left({}_{t_0}D_t^{\alpha+1}e(t)\right)|\dot{e}|^{1-\eta}\right) \tag{32}$$

u_{eq} Serves as the corresponding control element for operating the nominal component of the system.

$$u_{\text{SW}} = -\frac{1}{g_0(x,t)}(K_1 s + K_2 sign(s) + \Delta_D) \tag{33}$$

The robust control item u_{SW} is designed to effectively manage the lumped uncertainty $\Delta(x,t)$. The theorem presented below demonstrates that the convergence speed of surface Eq. (30) surpasses that of the integer-order terminal sliding mode control, as defined by Eq. (19).

- *Stability Analysis*

To prove the stability of the proposed control system, we first define the Lyapunov function as follows:

$$V = (1/2)s^2 \tag{34}$$

By taking the derivative of V with respect to time and using Eq. (31), we get:

$$\begin{aligned} \dot{V} &= s\dot{s} \\ &= s\left({}_{t_0}D_t^{\alpha+1}e(t) + \frac{\eta}{\lambda}|\dot{e}|^{\eta-1}(f_0(x,t) + g_0(x,t)u + \Delta(x,t) - \ddot{x}_d)\right) \\ &= s\left({}_{t_0}D_t^{\alpha+1}e(t) + \frac{\eta}{\lambda}|\dot{e}|^{\eta-1}(f_0(x,t) - \ddot{x}_d + \Delta(x,t))\right) + \frac{\eta}{\lambda}|\dot{e}|^{\eta-1}g_0(x,t)u \end{aligned} \tag{35}$$

It is possible to demonstrate that $\dot{V} \leq 0$ as long as the switching gain $|\Delta(x,t)| < \Delta_D$. By replacing the Eq. (32) and Eq. (34) with Eq. (35), we get:

$$\begin{aligned} \dot{V}(s) &= s\frac{\eta}{\lambda}|\dot{e}|^{\eta-1}\left(\Delta(x,t) - (K_1 s + K_2 sign\,(s) + \Delta_D)\right) \\ &\leq s\frac{\eta}{\lambda}|\dot{e}|^{\eta-1}\left(|\Delta(x,t)| - (K_1 s + K_2 sign\,(s) + \Delta_D)\right) \\ &\leq \frac{\eta}{\lambda}|\dot{e}|^{\eta-1}(-sK_1 s - K_2|s|) \leq 0 \end{aligned} \tag{36}$$

Therefore, according to Theorem 1 the system states will asymptotically approach $s(t) = 0$. Subsequently, we demonstrate that the discrepancy in tracking diminishes to zero within a finite time. Let t_r represent the time it takes for the system states to reach the sliding surface. This time may be approximated using Eq. (36), which specifies that $\dot{V}(s) = s\dot{s} \leq -(\eta K/\lambda)|s|$, where $K = max\{K_1, K_2\}$. By integrating $\dot{V}(t)$ with regard

to the final time $t = t_r$ and observing that $s(0) = 0$, the value of t_r can be determined as $t_r \leq |\lambda s(0)/\eta K|$. Consider $S_r = inf\{t \geq t_r : e(t) = 0\}$ as a stopping time for the states of the system. Next, we demonstrate the existence of a $t_s \in [t_r, \infty)$ that satisfies $S_r \leq t_s$. Specifically, by applying the fractional integral to both sides of Eq. (30) throughout the time interval from t_r to t, we get [27]:

$$\begin{aligned} &{}_{t_r}I_t^{\alpha}\left({}_{t_r}D_t^{\alpha}e(t)\right) \\ &= e(t) - {}_{t_r}D_t^{\alpha-1}e(t)\big|_{t=t_r}\frac{(t-t_r)^{\alpha-1}}{\Gamma(\alpha)} \\ &= -\frac{1}{\lambda_{t_r}}I_t^{\alpha}|\dot{e}(t)|^{\eta} \end{aligned} \tag{37}$$

Where ${}_{t_r}D_t^{\alpha-1}e(t)|_{t=t_r}((t-t_r)^{\alpha-1}/\Gamma(\alpha)) = 0$. By using the norm property, denoted as $\| \gamma u \| = |\gamma| \| u \|$, for $\gamma \in R$, and employing the outcome of Lemma 1, ($\| {}_{t_r}I_t^{\alpha}|\dot{e}(t)|^{\eta}\| \leq B\||\dot{e}(t)|^{\eta}\|$), we get:

$$\| e(t) \| \leq \frac{B}{\lambda}\||\dot{e}(t)|^{\eta}\| \leq \frac{B}{\lambda}\| \dot{e}(t) \|^{\eta} \tag{38}$$

Where B and λ are constants with positive values. By performing the integral of both sides of Eq. (38) with respect to the integer order from the time t_r to $t_s \in [t_r, \infty)$, we may get the following result [27]:

(39)

$$\begin{aligned} \left|\int_{t_r}^{t_s}\left(\frac{\lambda}{B}\right)^{1/\eta}ds\right| &\leq \left|\int_{t_r}^{t_s}\frac{d(\| e(s) \|)}{\| e(s) \|^{1/\eta}}\right| \Rightarrow t_s - t_r \\ &\leq \left(\frac{B}{\lambda}\right)^{1/\eta}\frac{\eta}{\eta-1}\left|\|e(t_s)\|^{1-\frac{1}{\eta}} - \|e(t_r)\|^{1-\frac{1}{\eta}}\right| \end{aligned}$$

(40)

$$t_s \leq \left(\frac{B}{\lambda}\right)^{1/\eta}\frac{\eta}{\eta-1}\|e(t_r)\|^{1-\frac{1}{\eta}} + t_r$$

Thus, it follows that the tracking error approaches zero at the finite time and so concludes the proof of stability.

Remark 1: It is important to highlight that to effectively manage significant uncertainties and external disturbances, the value of the switching item K_2 in controller Eq. (33) has to be substantial. This leads to a significant occurrence of chattering phenomena. In previous studies, many other functions have been suggested to replace the sign function to reduce chattering. Among these alternatives, we use the function $\frac{S}{\sqrt{S^2+1}}$ as a replacement for the sign function.

4. FINITE TIME DISTURBANCE OBSERVER DESIGN

For a second-order nonlinear system with a generic dynamics equation in the form of Eq. (13), the TSOM design is as follows [18,24-26]:

(41)

$$\begin{aligned} \dot{\hat{x}}_1 &= \rho_1|x_1 - \hat{x}_1|^{2/3}\text{sign}\,(x_1 - \hat{x}_1) + \hat{x}_2 \\ \dot{\hat{x}}_2 &= f_0(\hat{x}) + g_0(\hat{x})u + \rho_2|x_1 - \hat{x}_1|^{1/3}\text{sign}\,(x_1 - \hat{x}_1) - \\ \dot{\hat{\varphi}} &= -\rho_3\,\text{sign}(x_1 - \hat{x}_1) \end{aligned}$$

Where $\hat{x}$ is the estimation of x and ρ_i represents the observer's gains. The estimation error can be obtained by dividing the Eq. (13) and Eq. (41) as follows:

(42)

$$\begin{aligned} \dot{\tilde{x}}_1 &= -\rho_1|\tilde{x}_1|^{2/3}\text{sign}\,(\tilde{x}_1) + \tilde{x}_2 \\ \dot{\tilde{x}}_2 &= -\rho_2|\tilde{x}_1|^{1/3}\text{sign}\,(\tilde{x}_1) + \Delta(x,u,t) - d(x,\tilde{x},u,t) + \\ \dot{\tilde{\varphi}} &= -\rho_3\text{sign}\,(\tilde{x}_1) \end{aligned}$$

Where $\tilde{x} = x - \hat{x}$ represents the estimation error of the system states and the uncertainty estimation error function is written as follows:

(43)

$$\begin{cases} d(x,\tilde{x},u) = \{f_0(\hat{x}) + g_0(\hat{x})u\} - \{f_0(x) + g_0(x)u\} \\ \hat{\Delta}(x,\hat{x},u,t) = \Delta(x,u,t) - d(x,\tilde{x},u,t) \end{cases}$$

It is important to acknowledge that the error of estimating uncertainty is expected to be limited by $\| d(x,\tilde{x},u,t) \| \leq \Upsilon$.

Hence, the observer equation expressed in equation (21) may be restated as:

$$\begin{aligned} \dot{\hat{x}}_1 &= -\rho_1|\tilde{x}_1|^{2/3}\text{sign}\,(\tilde{x}_1) + \tilde{x}_2 \\ \dot{\hat{x}}_2 &= -\rho_2|\tilde{x}_1|^{1/3}\text{sign}\,(\tilde{x}_1) + \hat{\Delta}(x,\hat{x},u,t) + \hat{\varphi} \\ \dot{\hat{\varphi}} &= -\rho_3\text{sign}\,(\tilde{x}_1) \end{aligned} \tag{44}$$

The observer equation may be expressed by introducing the new variable $\hat{\varphi}_0 = \hat{\Delta}(x,\hat{x},u,t) + \hat{\varphi}$ as follow:

$$\begin{aligned} \dot{\tilde{x}}_1 &= -\rho_1|\tilde{x}_1|^{2/3}\text{sign}\,(\tilde{x}_1) + \tilde{x}_2 \\ \dot{\tilde{x}}_2 &= -\rho_2|\tilde{x}_1|^{1/3}\text{sign}\,(\tilde{x}_1) + \hat{\varphi}_0 \\ \dot{\hat{\varphi}}_0 &= -\rho_3\,\text{sign}(\tilde{x}_1) + \dot{\hat{\Delta}}(x,\hat{x},u,t) \end{aligned} \tag{45}$$

The equation provided represents the TOSM observer in its ultimate form, referred to as the

standard form of the second-order robust exact differentiator. This form ensures finite temporal stability, as shown in references [17-20]. By appropriately selecting the parameter values of the observer, the estimated errors of the states and uncertainties of the system will reach a value of zero within a limited amount of time. The settings for the TOSM observer may be chosen based on the findings of the research referenced in [17] in the following manner:

$$\begin{cases} \rho_1 = \lambda_1 L^{1/3}, \rho_2 = \lambda_2 L^{2/3}, \rho_3 = \lambda_3 L \\ \lambda_1 = 2, \lambda_2 = 2.12, \lambda_3 = 1.1 \\ L = \Lambda + \Upsilon \end{cases} \quad (46)$$

To calculate the uncertainty function of the system, it is essential to acknowledge that once the observer converges, the estimated state values will correspond to the actual state values of the system. Consequently, the error function used to estimate uncertainty will converge to zero ($\hat{x}_1 = x_1, \hat{x}_2 = x_2 \rightarrow d(x, \tilde{x}, u, t) = 0$).

Hence, the third component of the observer's equation may be expressed in the following manner:

$$\dot{\hat{\varphi}}_0 = -\rho_3 \text{sign}\,(\tilde{x}_1) + \dot{\hat{\Delta}}(x, \hat{x}, u, t) \equiv 0 \quad (47)$$

Hence, the calculation of the system's uncertainty estimation function may be determined in the following manner:

$$\hat{\Delta}(x, \hat{x}, u, t) = \int \rho_3 \text{sign}\,(\tilde{x}_1) \quad (48)$$

Given that the uncertainty function estimation in Eq. (48) has an integral component, the use of a low-pass filter is unnecessary for reconstructing the uncertainty estimation from the output injection term. The exceptional attribute of the TOSM observer enables more accurate estimations compared to conventional sliding mode-based observers.

To simulate the designed FTDO-based control system and its implementation, as well as to prove the stability, it is enough to insert the values obtained from the observer related to states and disturbance (lumped uncertainty) into the equations related to the controller design.

The issue that needs to be taken into consideration here is related to the interaction between the stability type of the observer and the controller. If the observer used in a control structure has asymptotic stability and the designed control system has finite time stability, it is possible that the control system as a whole does not have finite time stability. Therefore, after proving the stability of the observer and controller separately, the stability of the control system set should be checked once again considering the estimated values for the states and uncertainties of the system. Also, if the observer used has finite time stability, it will provide the guarantee that the estimated values of the system states will converge to the real values of the system states after a finite time and will be equivalent. Therefore, there is no need to prove the stability of the control system by placing the estimated values of the system states and uncertainties obtained from the observer [26]. In the current research, considering that the observer used is of the third-order sliding mode type and has finite time stability, therefore, re-proving the stability of the presented control system in combination with the observer will not be required, and proving the stability of the observer and controller independently of each other is sufficient.

Remark 2. One of the important points about fractional-order controllers is the challenge of their practical implementation. Given that the process of calculating fractional-order derivatives is different and more complex than natural-order derivatives, the question arises whether these methods can be implemented in practice, regardless of the results obtained from theoretical simulations. In recent years, considerable efforts have been made by researchers for this purpose, and fractional-order controllers have been successfully tested in practice in controlling various dynamic systems, and similar results have been obtained with the results obtained from theoretical simulations. As an example, we can refer to the research conducted in [13-15]. Therefore, based on the research conducted, it can be said that in the problem of controlling the attitude of satellites, the advantages of fractional-order control methods can be used in practice to improve tracking accuracy, convergence speed, and control system robustness. In this study, the simulations were designed to incorporate realistic satellite dynamics, including parametric uncertainties and external disturbances, as encountered in actual missions. The inclusion of these factors ensures that the testing conditions closely emulate practical scenarios. The proposed fractional-order sliding mode controller (FOSMC) and third-order sliding mode disturbance observer (TOSMDO) are designed to be computationally

efficient and implementable on existing satellite onboard processors. The methods primarily rely on measurable or estimable states, making them practical for real-time operations. Additionally, the robustness of FOSMC to parametric uncertainties and disturbances is advantageous for satellites operating in uncertain and varying conditions. While fractional-order controllers may introduce additional computational complexity compared to integer-order controllers, advancements in onboard computational capabilities and optimized algorithms can mitigate these concerns. Moreover, the third-order sliding mode disturbance observer relies on high-gain properties, which are sensitive to measurement noise. This challenge can be addressed by using appropriate noise-filtering techniques or sensor fusion approaches.

5. SIMULATION AND RESULTS

This segment comprises a simulation that demonstrates the functionality and effectiveness of the suggested controller. Because the outcomes of the proposed method will be juxtaposed with those of reference [14], the following simulation parameters and attitude reference signals are selected:

$$\sigma_d = 0.5[\sin(0.01t), -\cos(0.01t), \sin(0.01t)]^T$$
$$\sigma(0) = [0.7 \quad 0.5 \quad -0.3]^T$$
$$\omega(0) = [-0.001 \quad 0.001 \quad -0.001]^T \text{rad/s}$$
$$J = \begin{bmatrix} 3.06 & 1 & 0.4 \\ 1 & 3 & 1 \\ 0.4 & 1 & 3.95 \end{bmatrix}$$

For the simulation conditions to be close to reality, the uncertainty term and external disturbances are considered thoroughly, and a random term is also considered for unmodeled factors as follows:

$$d(t) = \begin{bmatrix} 0.06 - 0.04\sin(\omega_o t) + 0.05\cos(\omega_o t) \\ 0.07 + 0.05\sin(\omega_o t) - 0.04\cos(\omega_o t) \\ 0.04 - 0.03\sin(\omega_o t) + 0.03\cos(\omega_o t) \end{bmatrix} + 0.25 \times rand(3,1)(N \cdot m)$$

Where $\omega_o = \sqrt{\mu_g / \|\boldsymbol{r}\|^3}$ and $\mu_g = 3.986 \times 10^{14} (\text{m}^3/\text{s}^2)$.

The simulation results of the proposed control approach are depicted in Fig. 1–7, which are compared to the results reported in reference [14]. The tracking performance is satisfactory, as illustrated in the figures, and the control method outlined in this research surpasses the approach described in reference [14] concerning both tracking and control input performance. Fig. 1 and Fig. 2 show the position-tracking performance of the proposed control system and the position-tracking errors, and Fig. 3 and Fig. 4 show the velocity-tracking performance and the velocity-tracking errors, respectively. According to the results, it is clear that the FONTSMC control method combined with FTDO has a better performance than other used methods. The important point that can be taken from the obtained results is that the use of FTDO reduces the tracking error and improves the performance of the system. Also, according to the results, it is clear that fractional order controllers have better accuracy and convergence speed than integer order controllers.

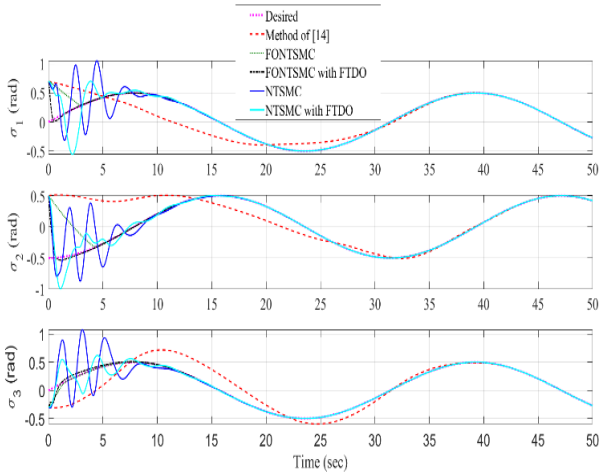

Fig. 1. Attitude tracking performance.

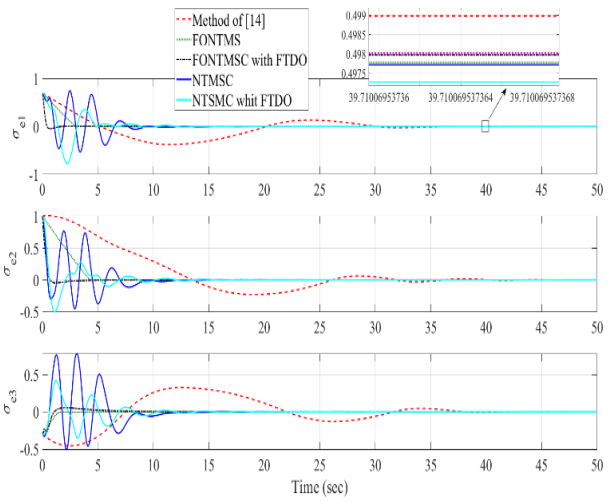

Fig. 2. Attitude tracking errors.

Figures 3 shows the results related to the time evolution of sliding surface functions and Fig. 4 shows the results related to the control inputs. Considering that the sign function in the control inputs was replaced with the function considered in Remark 1, the obtained results show that the obtained control inputs do not have chattering. Also, according to the results, it is clear that the control inputs related to a controller that uses the disturbance observer have a smaller domain, which is due to the accurate estimation of uncertainties and external disturbances entering the system and using the estimated values in the function of control inputs. The coefficient of the sign function for the stability of the control system is chosen in such a way that its value is greater than the system uncertainty function, which in the case of not using a disturbance observer, usually a large value is chosen as a precaution, which causes an increase in chattering and the range of control signals.

Therefore, the obtained results show the advantage of using disturbance observers in reducing the chattering phenomenon. The control inputs obtained in [14], although after reaching the stable state, have very small values, which are comparable in size to the control inputs obtained from the proposed control method, as can be seen in the obtained results, these signals have chattering that may damage the performance of the system drives in the long run.

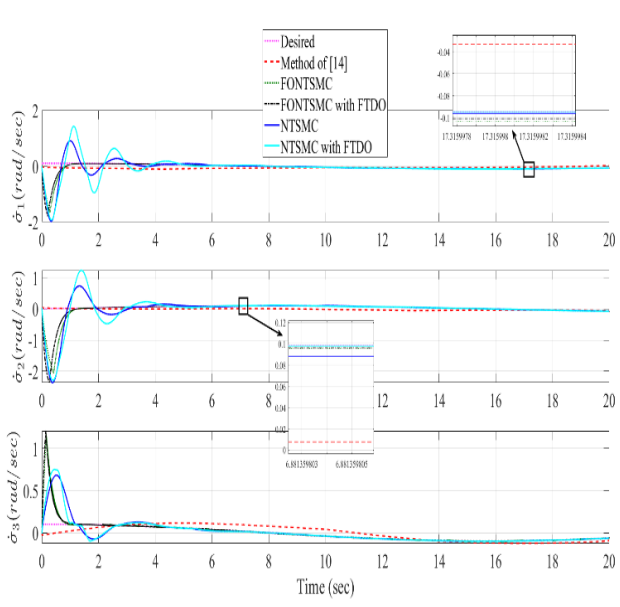

Fig. 3. Angular velocity tracking performance.

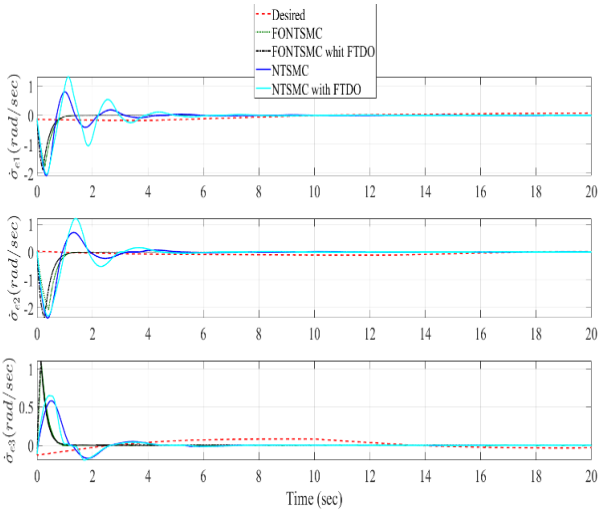

Fig. 4. Angular velocity tracking errors.

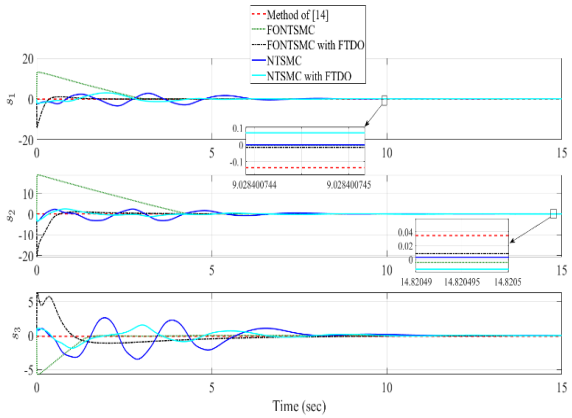

Fig. 5. Sliding surfaces.

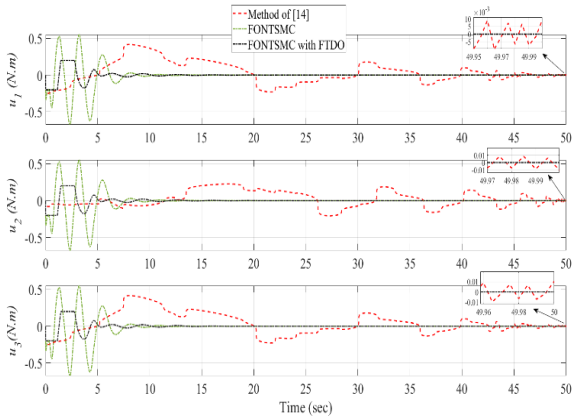

Fig. 6. Control inputs.

Figures 7 shows the performance results of the finite time disturbance observer in estimating system velocities. According to the obtained results, it is clear that the used observer has been able to estimate the states related to the velocities of the

system with high accuracy and reach convergence after a finite time.

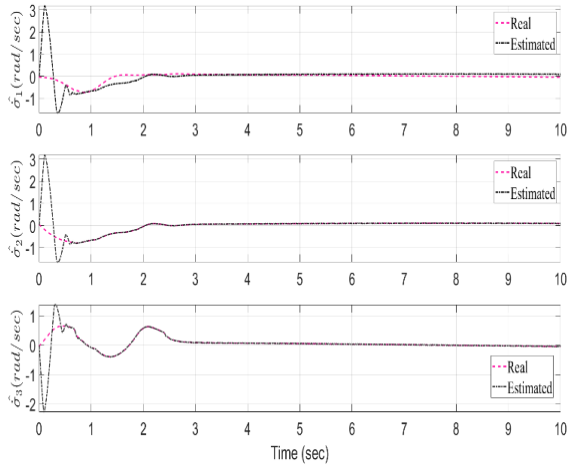

Fig. 7. FTDO observer performance in state estimation.

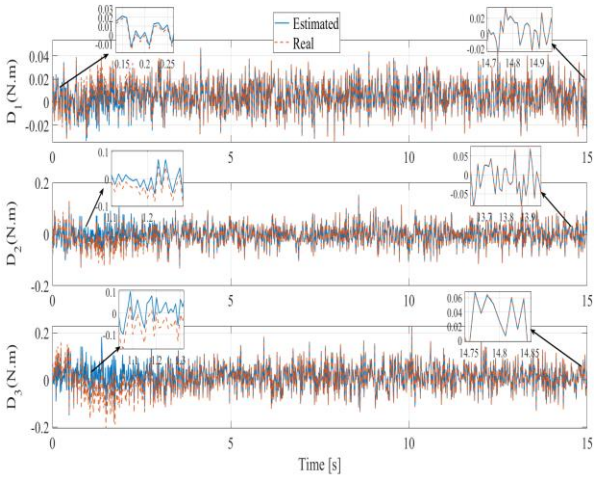

Fig. 8. FTDO observer performance in disturbance estimation.

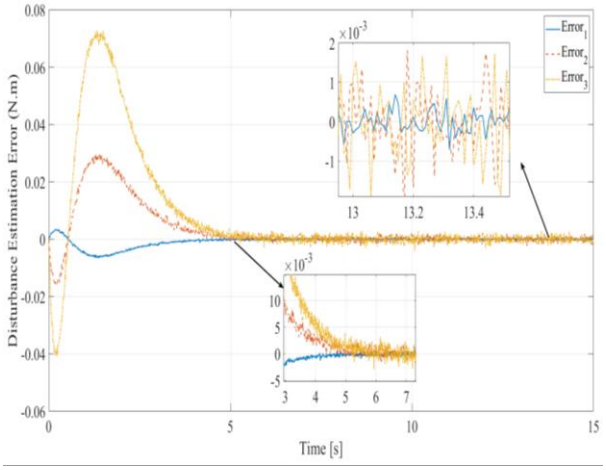

Fig. 9. FTDO observer's disturbance estimation errors.

Figures 8 and 9 show the performance of the designed disturbance observer in estimating the disturbance and uncertainty function and the estimation errors, respectively. As is clear from the figures, the observer has been able to estimate the external disturbances and uncertainty function with very high accuracy even in the presence of random noise. The steady-state error of the designed observer is of the order of 10^{-3}, which is considered to be very high accuracy. As previously stated, being resistant to noise was one of the important features of high-order sliding mode observers, and its objective performance can be seen here. This accurate estimation performance in the controller structure improves the tracking accuracy and also makes the control signals smoother and eliminates the chattering phenomenon.

6. CONCLUSIONS

This paper proposes a finite-time stable, fast convergent, and chattering-free attitude control system that does not need angular velocity data. For building an attitude controller, we utilized fractional order NTSMC in conjunction with FTDO (TOSM observer). The simulation results demonstrate the efficacy of the suggested strategy for rigid spacecraft attitude control. The obtained results indicate a very positive effect of using the proposed observer in improving the quality of control input signals as well as improving the accuracy of controller tracking due to the use of fractional order derivatives. The proposed methods have been developed with practical satellite operations in mind and tested under realistic conditions. We are confident that with appropriate engineering adaptations, the performance demonstrated in simulations can be realized in domestic satellite design and projects. To further validate the practical applicability of the proposed methods, future work will involve hardware-in-the-loop (HIL) simulations and real-world testing using small satellite platforms. These tests will provide additional insights into the implementation challenges and fine-tuning required for real missions.

CONFLICT OF INTERESTS

No conflict of interest has been expressed by the authors.

REFERENCES

[1] N. Nazari, H. Moladavoudi, and J. Beyramzad, "Finite time sliding mode control for agile rigid satellite with CMG actuators using fast high-order sliding mode observer," *Aerospace Systems*, vol. 7, pp. 363-383, 2024, https://doi.org/10.1007/s42401-024-00283-4.

[2] Y. Guo, B. Huang, J. H. Guo, A. J. Li, and C. Q. Wang, "Velocity-free sliding mode control for spacecraft with input saturation," *Acta Astronautica*, vol. 154, pp. 1-8, 2019, https://doi.org/10.1016/j.actaastro.2018.10.045.

[3] K. Zhang, G. R. Duan, and M. D. Ma, "Dynamic output feedback sliding mode control for spacecraft hovering without velocity measurements," *Journal of the Franklin Institute*, vol. 356, no. 4, pp. 1991-2014, 2019, https://doi.org/10.1016/j.jfranklin.2019.01.030.

[4] L. Yuan, G. Ma, C. Li, and B. Jiang, "Finite-time attitude tracking control for spacecraft without angular velocity measurements," *Journal of Systems Engineering and Electronics*, vol. 28, no. 6, pp. 1174-1185, 2017, https://doi.org/10.21629/JSEE.2017.06.15.

[5] Q. Hu and B. Jiang, "Continuous finite-time attitude control for rigid spacecraft based on angular velocity observer," *IEEE Transactions on Aerospace and Electronic Systems*, vol. 54, no. 3, pp. 1082-1092, 2017, https://doi.org/10.1109/TAES.2017.2773340.

[6] M. Malekzadeh and H. Sadeghian, "Attitude control of spacecraft simulator without angular velocity measurement," *Control Engineering Practice*, vol. 84, pp. 72-81, 2019, https://doi.org/10.1016/j.conengprac.2018.11.011.

[7] Y. Shtessel, C. Edwards, L. Fridman, and A. Levant, *Sliding Mode Control and Observation*, New York: Springer, 2014, https://doi.org/10.1007/978-0-8176-4893-0.

[8] J. Liu and X. Wang, *Advanced Sliding Mode Control for Mechanical Systems: Design, Analysis and MATLAB Simulation*, Berlin: Springer, 2012, https://doi.org/10.1007/978-3-642-20907-9.

[9] V. Shahbahrami, M. Azimi, and A. Alikhani, "Attitude and vibration control of a flexible spacecraft using hybrid adaptive super-twisting non-singular terminal sliding mode control," *Journal of Space Science and Technology*, vol. 16, no. 4, pp. 1-13, 2021, https://doi.org/10.30699/jsst.2023.1365.

[10] V. Utkin, A. Poznyak, Y. Orlov, and A. Polyakov, "Conventional and high order sliding mode control," *Journal of the Franklin Institute*, vol. 357, no. 15, pp. 10244-10261, 2020, https://doi.org/10.1016/j.jfranklin.2020.06.018.

[11] L. Fridman, J. A. Moreno, B. Bandyopadhyay, S. Kamal, and A. Chalanga, "Continuous nested algorithms: The fifth generation of sliding mode controllers," in *Recent Advances in Sliding Modes: From Control to Intelligent Mechatronics*: *Studies in Systems, Decision and Control 24*, X. Yu, and M. ÖnderEfe, Eds. Cham: Springer, 2015, pp. 5-35, https://doi.org/10.1007/978-3-319-18290-2_2.

[12] F. Shokouhi and A. H. Davaie Markazi, "A new continuous approximation of sign function for sliding mode control," in *6th International Conference on Robotics and Mechatronics (ICRoM 2018)*, Tehran, Iran, 2018.

[13] M. Navabi and M. R. Hosseini, "Investigation in to the effect of kinematic of the space craft attitude control using feedback linearization method," *Journal of Space Science and Technology*, vol. 11, no. 1, pp. 59-71, 2018.

[14] Y. Guo, B. Huang, S. M. Song, A. J. Li, and C. Q. Wang, "Robust saturated finite-time attitude control for spacecraft using integral sliding mode," *Journal of Guidance, Control, and Dynamics*, vol. 42, no. 2, pp. 440-446, 2019, https://doi.org/10.2514/1.G003520.

[15] M. Navabi and N. Safaei Hashekvaei, "Kinematic modelling without singularity and nonlinear control of satellite attitude using direct adaptive and fuzzy PD control methods," *Journal of Space Science and Technology*, vol. 14, no. 2, pp. 77-88, 2021, https://doi.org/10.22034/jsst.2021.1248.

[16] H. Yadegari, J. Beyramzad, and E. Khanmirza, "Magnetorquers-based satellite attitude control using interval type-II fuzzy terminal sliding mode control with time delay estimation," *Advances in Space Research*, vol. 69, no. 8, pp. 3204-3225, 2022, https://doi.org/10.1016/j.asr.2022.01.018.

[17] P. M. Tiwari, S. Janardhanan, and M. Nabi, "Attitude control using higher order sliding mode," *Aerospace Science and Technology*, vol. 54, pp. 108-113, 2016, https://doi.org/10.1016/j.ast.2016.04.012.

[18] M. Javaheripour, A. R. Vali, V. Behnam Gol, and F. Allahverdizadeh, "Design of an nonlinear extended state observer to estimate unmeasurable information on the problem of flying objects guidance," *Journal of Space Science and Technology*, vol. 15, no. 3, pp. 67-78, 2022, https://doi.org/10.30699/jsst.2022.1352.

[19] M. Alipour, M. Malekzadeh, and A. Ariaei, "Practical fractional-order nonsingular terminal sliding mode control of spacecraft," *ISA Transactions*, vol. 128, Part A, pp. 162-173, 2022, https://doi.org/10.1016/j.isatra.2021.10.022.

[20] Z. Ismail, R. Varatharajoo, and Y.C. Chak, "A fractional-order sliding mode control for nominal and underactuated satellite attitude controls," *Advances in Space Research*, vol. 66, no. 2, pp. 321-334, 2020, https://doi.org/10.1016/j.asr.2020.02.022.

[21] G. Zhao, "Fractional-order fast terminal sliding mode control for a class of dynamical systems," *Mathematical Problems in Engineering*, vol. 2013, no. 1, 2013, Art. no. 384921, https://doi.org/10.1155/2013/384921.

[22] C. A. Monje, Y. Q. Chen, B. M. Vinagre, D. Xue, and V. Feliu-Batlle, *Fractional-Order Systems and Controls: Fundamentals and Applications*, Springer, London, 2010.

[23] D. Xue, *Fractional-Order Control Systems: Fundamentals and Numerical Implementations*, Walter de Gruyter, 2017.

[24] V. C. Nguyen, A. T. Vo, and H. J. Kang, "A finite-time fault-tolerant control using non-singular fast terminal sliding mode control and third-order sliding mode observer for robotic manipulators," *IEEE Access*, vol. 9, pp. 31225-31235, 2021, https://doi.org/10.1109/ACCESS.2021.3059897.

[25] M. Van, H. J. Kang, Y. S. Suh, and K. S. Shin, "Output feedback tracking control of uncertain robot manipulators via higher-order sliding-mode observer and fuzzy compensator," *Journal of Mechanical Science and Technology*, vol. 27, pp. 2487-2496, 2013, https://doi.org/10.1007/s12206-013-0636-3.

[26] M. Van, P. Franciosa, and D. Ceglarek, "Fault diagnosis and fault-tolerant control of uncertain robot manipulators using high-order sliding mode," *Mathematical Problems in Engineering*, vol. 2016, no. 1, 2016, Art. no. 7926280, https://doi.org/10.1155/2016/7926280.

[27] T. M. Duc, N. V. Hoa, and T. P. Dao, "Adaptive fuzzy fractional-order nonsingular terminal sliding mode control for a class of second-order nonlinear systems," *Journal of Computational and Nonlinear Dynamics*, vol. 13, no. 3, 2018, Art. no. 31004, https://doi.org/10.1115/1.4038642.

[28] Y. Li, Y. Q. Chen, and I. Podlubny, "Mittag–Leffler stability of fractional order nonlinear dynamic systems," *Automatica*, vol. 45, no. 8, pp. 1965-1969, 2009, https://doi.org/10.1016/j.automatica.2009.04.003.

[29] D. Cao and J. Fei, "Adaptive fractional fuzzy sliding mode control for three-phase active power filter," *IEEE Access*, vol. 4, pp. 6645-6651, 2016, https://doi.org/10.1109/ACCESS.2016.2586958.

[30] A. A. Kilbas, H. M. Srivastava, and J. J. Trujillo, *Theory and Applications of Fractional Differential Equations*, 1st ed, Elsevie, 2006.

[31] G. Sun, L. Wu, Z. Kuang, Z. Ma, and J. Liu, "Practical tracking control of linear motor via fractional-order sliding mode," *Automatica*, vol. 94, pp. 221-235, 2018, https://doi.org/10.1016/j.automatica.2018.02.011.

[32] J. Fei and H. Wang, "Experimental investigation of recurrent neural network fractional-order sliding mode control of active power filter," *IEEE Transactions on Circuits and Systems II: Express Briefs*, vol. 67, no. 11, pp. 2522-2526, 2019, https://doi.org/10.1109/TCSII.2019.2953223.

[33] C. Izaguirre-Espinosa, A. J. Muñoz-Vázquez, A. Sánchez-Orta, V. Parra-Vega, and P. Castillo, "Attitude control of quadrotors based on fractional sliding modes: Theory and experiments," *IET Control Theory & Applications*, vol. 10, no. 7, pp. 825-832, 2016, https://doi.org/10.1049/iet-cta.2015.1048.

[34] H. P. Ren, X. Wang, J. T. Fan, and O. Kaynak, "Fractional order sliding mode control of a pneumatic position servo system," *Journal of the Franklin Institute*, vol. 356, no. 12, pp. 6160-6174, 2019, https://doi.org/10.1016/j.jfranklin.2019.05.024.

[35] S. Li, H. Lu, J. Li, T. Zheng, and Y. He, "Fractional-order sliding mode controller based on ESO for a buck converter with mismatched disturbances: Design and experiments," *IEEE Transactions on Industrial Electronics (Early Access)*, pp. 1-12, 2025, https://doi.org/10.1109/TIE.2024.3525110.